High preseason temperature variability drives convergence of xylem phenology in the Northern Hemisphere conifers

High preseason temperature variability drives convergence of xylem phenology in the Northern Hemisphere conifers

Yaling Zhang[1], Jian-Guo Huang[2*], Minhuang Wang[3], Wenjin Wang[1], Annie Deslauriers[4], Patrick Fonti[5], Eryuan Liang[6], Harri Mäkinen[7], Walter Oberhuber[8], Cyrille B. K. Rathgeber[9], Roberto Tognetti[10], Václav Treml[11], Bao Yang[12], Lihong Zhai[2], Serena Antonucci[10], Valentina Buttò[13], J. Julio Camarero[14], Filipe Campelo[15], Katarina Čufar[16], Martin De Luis[17], Marek Fajstavr[18], Alessio Giovannelli[19], Jožica Gričar[20], Andreas Gruber[8], Vladimír Gryc[18], Aylin Güney[21], Tuula Jyske[7], Jakub Kašpar[11, 22], Gregory King[5, 23], Cornelia Krause[4], Audrey Lemay[4], Fabio Lombardi[24], Edurne Martínez del Castillo[17], Hubert Morin[4], Cristina Nabais[15], Pekka Nöjd[7], Richard L. Peters[5, 25], Peter Prislan[20], Antonio Saracino[26], Vladimir V. Shishov[27], Irene Swidrak[8], Hanuš Vavrčík[18], Joana Vieira[15], Qiao Zeng[28], and Sergio Rossi[5]

Affiliations:

[1] Key Laboratory of Vegetation Restoration and Management of Degraded Ecosystems, Guangdong Provincial Key Laboratory of Applied Botany, South China, Botanical Garden, Chinese Academy of Sciences, 723 Xingke Road, Tianhe District, Guangzhou, 510650, China

[2] MOE Key Laboratory of Biosystems Homeostasis and Protection, College of Life Sciences, Zhejiang University, Hangzhou 310058, China

[3] Department of Ecology, School of Life Sciences, State Key Laboratory of Biocontrol, Sun Yat-sen University, Guangzhou, 510275, China

[4] Laboratoire sur les écosystèmes terrestres boréaux, Département des Sciences Fondamentales, Université du Québec à Chicoutimi, Chicoutimi (QC), Canada

[5] Swiss Federal Research Institute for Forest, Snow and Landscape Research WSL, Zürcherstrasse 111, CH-8903 Birmensdorf, Switzerland

[6] Key Laboratory of Alpine Ecology and Biodiversity, Key Laboratory of Tibetan Environment Changes and Land Surface Processes, Institute of Tibetan Plateau Research, Chinese Academy of Sciences, Beijing, China

[7] Natural Resources Institute Finland, Latokartanonkaari 9, 00790 Helsinki, Finland

[8] Department of Botany, Leopold-Franzens-University of Innsbruck, Innsbruck, Austria

[9] Université de Lorraine, AgroParisTech, INRAE, Silva, F-54000 Nancy, France

[10] Dipartimento di Agricoltura, Ambiente e Alimenti, Università degli Studi del Molise, Campobasso, 86100, Italy

[11] Department of Physical Geography and Geoecology, Charles University, Prague, CZ-12843, Czech Republic

[12] School of Geograph and Oceanograph Sciences, Nanjing University, Nanjing 210093, China

[13] Forest Research Institute, Université du Quebec en Abitibi-Témiscamingue, Rouyn-Noranda, Quebec, Canada J9X5E4

[14] Instituto Pirenaico de Ecología (IPE-CSIC), Avda. Montañana 1005, Zaragoza, 50192, Spain

[15] Centre for Functional Ecology, Department of Life Sciences, University of Coimbra, Calçada Martim de Freitas, Coimbra, 3000–456, Portugal

[16] University of Ljubljana, Biotechnical Faculty, Ljubljana, Slovenia

[17] Department of Geography and Regional Planning, Environmental Science Institute, University of Zaragoza, Zaragoza, 50009, Spain

[18] Department of Wood Science and Wood Technology, Mendel University in Brno, Zemědělská 3, Brno, 61300, Czech Republic

[19] CNR – Istituto di Ricerca sugli Ecosistemi Terrestri, IRET, Sesto Fiorentino, Italy

[20] Slovenian Forestry Institute, Ljubljana, Slovenia

[21] Izmir Katip Çelebi University, Faculty of Forestry, Izmir, Turkey

[22] Silva Tarouca Research Institute for Landscape and Ornamental Gardening, Department of Forest Ecology, 252 43 Průhonice, Czech Republic
[23] Department of Sciences, University of Alberta, Camrose, AB, Canada
[24] AGRARIA Department, Mediterranean University of Reggio Calabria, 89124, Italy
[25] Physiological Plant Ecology, Department of Environmental Sciences, University of Basel, Schönbeinstrasse 6, CH-4056 Basel, Switzerland
[26] Department of Agricultural Sciences, University of Naples Federico II, I-80055 Portici-Napoli, Italy
[27] Institute of Economics and Trade, Siberian Federal University, Krasnoyarsk, 660075, Russia
[28] Key Lab of Guangdong for Utilization of Remote Sensing and Geographical Information System, Guangdong Open Laboratory of Geospatial Information Technology and Application, Guangzhou Institute of Geography, Guangzhou 510070, China
Keywords:
Cell differentiation, Northern Hemisphere, spring forcing, winter chilling, wood formation, 5th of June.
Correspondence
jianguo.huang@zju.edu.cn

Summary

Wood growth is key to understanding the feedback of forest ecosystems to the ongoing climate warming. An increase in spatial synchrony (i.e., coincident changes in distant populations) of spring phenology is one of the most prominent climate responses of forest trees. However, whether temperature variability contributes to an increase in the spatial synchrony of spring phenology and its underlying mechanisms remain largely unknown. Here, we analyzed an extensive dataset of xylem phenology observations of 20 conifer species from 75 sites over the Northern Hemisphere. Along the gradient of increase in temperature variability in the 75 sites, we observed a convergence in the onset of cell enlargement roughly toward the 5th of June, whereas a convergence in the onset of cell wall thickening toward the summer solstice. The increase of rainfall since the 5th of June is favorable for cell division and expansion, and the most hours of sunlight around the summer solstice allows optimizing carbon assimilation for cell wall thickening. Hence, the convergences can be considered as the result of matching xylem phenological activities into favorable conditions in regions with high temperature variability. Yet, forest trees relying on such consistent seasonal cues for xylem growth could constrain their ability to respond to climate warming, with consequences for the potential growing season length and ultimately forest productivity and survival in the future.

Introduction

Wood formation in forest trees involves the progression from cell enlargement to cell wall thickening, lignification, and programmed cell death [1], and the carbon allocated to long-lived woody tissues stays in the ecosystem for decades to centuries [2,3]. Given warming-induced decoupling between growth timing and annual woody growth [3], the subtle responses of wood formation (e.g., xylem phenology) to multiple facets of global warming should be quantified to improve our understanding of forest growth dynamics; however, this task remains challenging. One of the largest uncertainties in the responses of wood formation to global warming is the inferences derived solely from mean annual temperatures [4-6]. However, temperature fluctuates at various time scales, including daily and seasonal variations [7,8]. The prediction of future xylem phenological shifts requires knowledge of the effects of temperature variability on the timing of xylem spring phenology; however, such knowledge is scarce at large spatial scales [9,10], and the underlying mechanisms remain to be quantified.

Previous attempts to explicitly link spring phenology to local temperature variability have assumed that large variations in spring temperature cause high frost risk [9]. In such unpredictable climates, simply following temperatures at the "wrong" time of the year causes fatal consequences for forest trees, being particularly dangerous for tree populations growing in seasonally cold climates. Tree species are under continuous selective pressure to match their phenology to favorable environmental conditions to minimize the risk of frost damage [11]. The selection pressure from frost risk should drive plants to rely on consistent, reliable seasonal cues that could provide favorable environmental conditions to initiate the xylem spring phenological phases.

The spring resumption of cambium activity requires the information that winter has passed, obtained from the dose of low temperatures experienced by the forest trees [12]. A growing body of hypotheses has suggested that forest trees would extend the duration of chilling exposure [10,13], so that wait until the risk of frost damage has passed in climates with high temperature variability. It has been reported that chilling temperatures between −5 °C and 5 °C are most effective for the onset of cambium activity [5]. However, larger variations in spring temperature may increase the probability of exceeding this chilling temperature range (−5 °C and 5 °C), lowering chilling accumulation. As such, if forest trees avoid frost damage via extending chilling exposure when temperature variability is high?

In this study, we leveraged the developments in microsampling wood approaches that enable the direct monitoring of xylem phenology [14]. We compiled a large dataset of weekly observations of xylem cell enlargement and cell wall thickening of 20 conifer species from 75 sites distributed throughout the Northern Hemisphere across boreal, temperate, Mediterranean, and subtropical biomes (Fig. S1 and Table S1). Utilizing this unique high-temporal-resolution data set, we aimed to provide the first spatial pattern of the onset dates of xylem cell enlargement and wall thickening along the gradients of temperature variability across the 75 sites, and to elucidate if forest trees rely on consistent, reliable seasonal cues to start the xylem growth in regions with high temperature variability. If yes, then what are the seasonal cues and what are the underlying mechanisms?

Results

Convergence in the onset of xylem spring phenology with the increase in temperature variability (PTV) across the sites

The slopes of the different quantile regressions of the PTV with the onset dates of cell enlargement ($Cell_e$ DOY) and wall thickening ($Cell_w$ DOY) across all preseason periods are

shown in Figs. S3–4. Convergences in the responses of xylem cell enlargement and cell wall thickening with the increase in PTV across the 75 sites in the current study were observed (Figs. S3–4). With an increase in the PTV, we observed a convergence in the $Cell_e$ DOY roughly toward the 5th of June, whereas a convergence in the $Cell_w$ DOY occurred near the summer solstice (Figs. 1a–b). Rainfall increased since the 5th of June as shown by significantly higher mean daily precipitation (Fig. 2). The slopes varied across these different quantiles: in the lower quantiles, where the $Cell_e$ DOY and $Cell_w$ DOY generally appeared in relatively warm areas, the PTVs were positively associated with the DOY (Figs. 1a–b). In contrast, in the higher quantiles, where $Cell_e$ DOY and $Cell_w$ DOY occurred in relatively cold regions, this relationship was negative (Figs. 1a–b). In addition, the steepest slopes were associated with the lowest and highest quantiles.

We defined the optimal preseason as the period, ranging between 20 and 140 days before the $Cell_e$ DOY and $Cell_w$ DOY, with 20-day steps, with the most convergence trend of the DOYs with the increase in PTV. The most convergence trend was selected by identifying the preseason period with the largest difference between the slopes of the highest and lowest quantiles for both cell enlargement and cell wall thickening. The preseason 80-day temperature variability (PTV_80) presented the most distinct slopes for both DOYs and was selected as the optimal preseason for analyses (Figs. S3–4).

Structural equation models (SEMs)

We selected the quantiles lower than the 15th quantile and higher than the 85th quantile of the $Cell_e$ DOY and $Cell_w$ DOY to represent early and late onset dates, respectively (Figs. 1a–b). The quantiles below the 15th one appeared in relatively warm areas, whereas the quantiles greater than the 85th corresponded to relatively cold regions (Figs. 3a–b).

Elevated PTV_80 generally increased frost days except for $Cell_e$ DOY in relatively cold regions, which was not statistically significant, as indicated by the standardized coefficients (Figs. 4a–d). Increased frost days were associated with later $Cell_w$ DOY in relatively warm regions but with earlier $Cell_w$ DOY in relatively cold regions (standardized coefficients of 0.45 and –0.81, respectively). In contrast, the increased frost days were associated with earlier $Cell_e$ DOY in relatively warm regions (standardized coefficients of –0.35) (Fig. 4a). Similarly, elevated PTV_80 generally accelerated forcing accumulation, except for $Cell_e$ DOY in relatively cold regions, which was not statistically significant (Figs. 4a–d). The accelerated forcing accumulation was associated with later $Cell_e$ DOY and $Cell_w$ DOY. In contrast, elevated PTV_80 generally decreased chilling accumulation for $Cell_e$ DOY, which was linked to earlier onset dates. Only for the $Cell_w$ DOY in relatively warm regions, chilling accumulation increased and was linked to later onset dates (Figs. 4a–d).

Discussion

Along the gradient of increase in temperature variability in the 75 sites across boreal, temperate, Mediterranean, and subtropical biomes, we observed a convergence in the onset of cell enlargement roughly toward the 5th of June, and a convergence in the onset of cell wall thickening toward the summer solstice (Figs. 1a–b). This indicated that, in regions with high temperature variability, forest trees prefer to rely on the 5th of June and the summer solstice to initiate xylem cell enlargement and wall thickening, respectively. The cambium resumption changes according to variations in environmental factors and is usually delayed at high altitudes and latitudes in comparison with low altitudes and latitudes [14]. Thus, the earlier spring phenological activities occurred in relatively warmer areas in comparison to the later ones [4],

which is also known as a phenomenon referred to as Hopkins' bioclimatic law [15]. However, our observation of the convergence in the onset of xylem growth indicated an increase in the spatial synchrony of xylem spring phenology with the increase in temperature variability (Figs. 1a–b). The increase in spatial synchrony in plant phenology has been increasingly reported across altitudes, latitudes, and urban–rural gradients [16-18]; however, to the best of our knowledge, this spatial synchrony has never been linked to increases in temperature variability. Sufficient water availability is necessary to support xylem cell division and expansion [19,20], and thus, the 5th of June, since when rainfall increased (Fig. 2), acts as a favorable seasonal cue for trees to initiate cell enlargement. In contrast, cell wall thickening is based on the supply of sugars [20], which are mainly regulated by carbon assimilation through photosynthesis [22,23]. Photosynthetic performance is more closely linked to the length of the day than to temperature; that is, warm short-day conditions reduce photosynthetic performance [24,25]. Summer solstice, during which the Northern Hemisphere receives the most hours of daylight, is the optimal time to maximize carbon assimilation [33]. Moreover, the 5th of June and the summer solstice provided relatively consistent seasonal cues for xylem cell enlargement and cell wall thickening and thus could prevent forest trees from simply tracking the unpredictable temperature signal in regions with high temperature variability. Therefore, the convergence on the 5th of June and the summer solstice exhibited by the onset dates of cell enlargement and cell wall thickening, respectively (Figs. 1a–b), can be considered as the result of matching xylem phenological activities into favorable environmental conditions.

Previous attempts to explicitly link spring phenology to local temperature variability have assumed that a large temperature range increases the probability of frost risk [9]. We observed consistent results showing that high temperature variability generally increases the number of frost days (Figs. 4a–d). Consequently, long-lived tree species are expected to have evolved "cautious" phenological strategies that onset the spring phenological activities later with higher temperature variability to avoid frost damage [25], which should be especially important in cold regions. Yet, we observed that forest trees initiate xylem growth earlier with higher temperature variability regardless of the increase in the number of frost days in relatively cold sites (Figs. 1a–b; Figs. 4b, d). This indicated that forest trees bear the risk of frost damage to initiate the xylem growth around the 5th of June and the summer solstice. It has also been proposed that tree species from regions with high temperature variability are expected to experience a longer period of chilling temperatures for dormancy release in spring until the risk of frost damage has passed [10]. However, our results indicated that forest trees in areas with high temperature variability generally experienced lower amounts of chilling temperatures (Figs. 4a–d). These findings contradict previous assumptions indicating that minimizing frost damage is the priority for forest trees to initiate xylem growth in regions with high temperature variability [9]. Instead, guiding the xylem growth activities into favorable amounts of precipitation and sunlight is the priority for forest trees located in areas with high temperature variability.

In areas with low temperature variability, the advent of xylem spring is rather variable over space, as indicated by the high overall variation in the onset dates of both xylem cell enlargement and cell wall thickening (Figs. 1a–b). However, in the context of increase in temperature variability under global warming [26], if forest trees would rely on the 5th of June for the onset of xylem cell enlargement and the summer solstice for the cell wall thickening, as such to guarantee favorable conditions in the future? If so, the xylem spring phenological activities that appeared in relatively warm regions could be potentially delayed and the ones in relatively cold areas could be advanced (Figs. 1 a–b and 3 a–b). We assume that the onset of xylem cell enlargement and wall thickening in extremely warm and cold regions are the most significantly affected phases (Figs. 1a–b). Our results question previous findings

indicating that increases in temperature variability would delay the onset of spring phenology [9,10]. In contrast, we propose a substantial variation in the direction and magnitude of the potential changes in the onset dates of xylem spring phenology in areas with low temperature variability.

By contrast, in areas with high temperature variability, forest trees adopt relatively consistent onset dates for both xylem cell enlargement and cell wall thickening (Figs. 1a–b), trees' phenological flexibility is therefore expected to be lower. Other studies have indicated that genotypes from harsher environments have less phenological flexibility than those from more mesic sites [16,27,28]. Thus, the low phenological flexibility of forest trees that rely on consistent seasonal cues despite climate warming in areas with high temperature variability, could potentially constrain the lengthening of the potential growing season, and ultimately forest productivity and survival in the future [27]. Further, due to the ongoing changes in global precipitation patterns [29], the low phenological flexibility of forest trees could bring trees into unfavorable conditions for cell enlargement in regards of water availability. By contrast, the onset of cell wall thickening has been reported to be less affected by precipitation [30], so that should not be affected. This implies potential mismatches between the xylem cell enlargement and wall thickening in the context of climate change. While xylem cell wall thickening is a process accounting for 90% of woody biomass production, cell enlargement is responsible for cell production, or size growth [31]. The decoupling therefore could potentially influence the fitness, structure and functioning of forest ecosystems, especially when interacting with local factors (e.g., geographic, edaphic and vegetational factors), and bring large uncertainty to carbon sinks in forests in areas with highly fluctuated temperatures. The low phenological flexibility is also highly linked to invasion success [32], migration potential for future populations and the ability to acclimate to the new thermal environment, and forest productivity and survival [25].

Conclusion

We provided empirical evidence to show an increase in spatial synchrony of xylem spring phenology with the increase in temperature variability across the 75 sites in the current study over the Northern Hemisphere, with the convergence of the xylem cell enlargement around the 5th of June, and wall thickening around the summer solstice. The 5th of June, since when rainfall increases, guarantees favorable amounts of precipitation for turgor-driven cell division and expansion, while the summer solstice with the most hours of sunlight is favorable for carbon assimilation and enhances cell wall thickening. We observed that forest trees even bear the risk of frost damage to initiate xylem growth earlier with higher temperature variability in relatively cold sites, to rely on the 5th of June for cell enlargement, and the summer solstice for cell wall thickening. It therefore suggests that guaranteeing favorable conditions is the priority for forest trees to initiate the xylem growth when temperature variability is high. In areas with low temperature variability, the advent of cell enlargement could be potentially guild into the 5th of June, and cell wall thickening into the summer solstice in future context of increasing temperature variability under global warming. By contrast, in regions with high temperature variability, forest trees rely on the fixed dates to initiate xylem growth, which could in turn constrain the ability of trees to respond to climate warming, consequently the lengthening of the potential growing season, and ultimately forest productivity and survival in future. Furthermore, due to the ongoing changes in global precipitation patterns, such low flexibility in xylem phenological strategies could bring trees into unfavorable conditions for cell enlargement, but not for the onset of cell wall thickening that is less affected by precipitation. This implies potential mismatches between the onsets of xylem cell enlargement and wall thickening, which consequently affect the fitness, structure and functioning of forest

ecosystems, in the context of climate change.

ACKNOWLEDGMENTS

We appreciate Constantin Zohner for providing valuable comments and suggestions on the manuscript. This work was funded by the National Natural Science Foundation of China (32271653, 32001138), the Xinjiang Regional Collaborative Innovation Project (2022E01045), and Zhejiang University (108000*1942222R1). Other funding agencies included the Austrian Science Fund (FWF P22280-B16; P25643-B16), Consortium de Recherche sur la Forêt Boréale Commerciale, Fonds de Recherche sur la Nature et les Technologies du Québec, Forêt d'enseignement et de recherche Simoncouche, Observatoire régional de recherche en forêt boréale, Natural Sciences and Engineering Research Council of Canada, Slovenian Research and Innovation Agency ARIS (research core funding Nos.: P4-0430 and P4-0015, projects: J4-2541, J4-4541 and Z4-7318), European Union's Horizon 2020 research and innovation program ASFORCLIC grant agreement N°952314, MIUR-PRIN 2002 (2002075152) and 2005 (2005072877), Swiss National Science Foundation (Projects INTEGRAL-121859 and LOTFOR-150205), French National Research Agency (ANR) as part of the "Investissements d'Avenir" program (ANR-11-LABX-0002-01, Lab of Excellence ARBRE), Academy of Finland (Nos. 250299, 257641 and 265504), NSFC (41525001), Grant Agency of Czech Republic (P504/11/P557), and Provincia Autonoma di Trento (project "SOFIE 2"–3012/2007). Cooperation among authors was supported by the EU COST Action FP1106 STReESS. The views and conclusions contained in this document are those of the authors and should not be interpreted as representing the opinions or policies of funding agencies and supporting institutions.

AUTHOR CONTRIBUTIONS

J.H. and Y.Z. designed this study. Y.Z. and M.W. analyzed the data. Y.Z. wrote the original manuscript with assistance from J.H. and S.R. All co-authors contributed to this work in various ways, including conducting field experiments, laboratory work, preprocessing, and contribution of data, and commenting on and improving the manuscript.

DECLARATION OF INTERESTS

The authors declare no competing interests.

FIGURE LEGENDS

Fig. 1. Cell enlargement day of the year (DOY) (A) and cell wall thickening DOY (B) as a function of the preseason temperature variability (PTV)

PTV is calculated as the standard deviation during a period of 80 days before the day of onset of cell enlargement and cell wall thickening, respectively, for each tree, site, and year). Model fits of Bayesian quantile regression analysis for multiple quantiles (1^{st}, 5^{th}, 10^{th}, 15^{th}, 25^{th}, 50^{th}, 75^{th}, 85^{th}, 90^{th}, 95^{th} and 99^{th} percentiles) are visualized as solid blue lines with credible intervals (95%) shown in gray. We also obtained the mean regression (denoted by the thick red line), which can be used as a central regression line similar to the mean regression estimated using ordinary least squares regression. The purple lines indicate the 5^{th} of June (A) and the summer solstice (B).

Fig. 2. Frequency distributions of the mean daily precipitation (MDP)

The MDP were calculated before the 5^{th} June (starts from the first day of year to the 5^{th} June)

and after 5th June (starts from the 6th June to the end of cell wall thickening).

Fig. 3. Frequency distributions of the mean annual temperature

The mean annual temperature were calculated for the values of the cell-enlargement day of the year (DOY) (a) and cell-wall-thickening DOY (b) lower than the 15th quantile and higher than the 85th quantile, respectively. Es: the onset dates of cell enlargement; Ws: the onset dates of cell wall thickening.

Fig. 4. Direct and indirect effects of the preseason temperature variability (PTV_80) on the cell-enlargement day of the year ($Cell_e$ DOY) and wall-thickening DOYs ($Cell_w$ DOY) based on their influences on frost days, chilling accumulation, and forcing accumulation.

(A) The SEM for $Cell_e$ DOY values below the 15th quantile, which represent 15% of earliest $Cell_e$ DOY; **(B)** The SEM for $Cell_e$ DOY values above the 85th quantile, which represent 15% of latest $Cell_e$ DOY; **(C)** The SEM for $Cell_w$ DOY values below the 15th quantile, which represent 15% of earliest $Cell_w$ DOY; **(D)** The SEM for $Cell_w$ DOY values above the 85th quantile, which represent 15% of latest $Cell_w$ DOY. PTV_80 is the PTV calculated as the standard deviation during a period of 80 days before the day of onset of cell enlargement and wall thickening for each tree, site, and year; The arrows illustrate the direction and magnitude of the paths; the solid red and green arrows represent significant positive and negative standardized path coefficients ($P < 0.05$), respectively, and the dashed arrows represent non-significant standardized path coefficients.

STAR+METHODS

Detailed methods are provided in the online version of this paper and include the following:

- KEY RESOURCES TABLE
- RESOURCE AVAILABILITY
  - Lead contact
  - Materials availability
  - Data and code availability
- EXPERIMENTAL MODEL AND SUBJECT DETAILS
- METHOD DETAILS
  - Field experiments and sample collection
  - Xylem phenology data
  - Climate data
  - Preseason chilling and forcing
  - Preseason temperature variability (PTV) and frost days
- QUANTIFICATION AND STATISTICAL ANALYSIS

SUPPLEMENTAL INFORMATION

Supplemental information can be found online at https://doi.org/10.1016/j.cub.2024. ##.###.

LEGEND for Data S1

Data S1. The sites, species, and years included in the analysis.

The species were reported with the following acronyms and classified into early (E) and late (L) successional species type: ABAL, *Abies alba*, L; ABBA, *Abies balsamea*, L; ABGE, *Abies georgei*, L; CELI, *Cedrus libani*, L; JUPR, *Juniperus przewalskii*, E; JUTH, *Juniperus thurifera*, E; LADE, *Larix decidua*, E; PCAB, *Picea abies*, L; PCMA, *Picea mariana*, L; PICE, *Pinus cembra*, L; PIHA, *Pinus halepensis*, E; PIHE, *Pinus heldreichii*, E; PILE, *Pinus leucodermis*, E; PILO, *Pinus longaeva*, E; PIMA, *Pinus massoniana*, E; PIPE, *Pinus peuce*, E; PIPI, *Pinus pinaster*, E; PISY,

Pinus sylvestris, E; PITA, *Pinus tabulaeformis*, E; and PIUN, *Pinus uncinata*, E. The entire study area was divided into subtropical (S), Mediterranean (M), temperate (T), and boreal (B) biomes. The temperature for each site was computed as the average of the MATs across all years for which observations were recorded for the site. The sites for which data was obtained from nearby weather stations are indicated by *.

REFERENCES

1. Begum, S., Nakaba, S., Yamagishi, Y., Oribe, Y., and Funada, R. (2013). Regulation of cambial activity in relation to environmental conditions: understanding the role of temperature in wood formation of trees. Physiol. Plant. *147*, 46-54. https://doi.org/10.1111/j.1399-3054.2012.01663.x.

2. Xue, B.-L., Guo, Q.H., Hu, T.Y., Xiao, J.F., Yang, Y.H. , Wang, G.Q, Tao, S.L., Su, Y.J., Liu, J., and Zhao, X.Q. (2017). Global patterns of woody residence time and its influence on model simulation of aboveground biomass, Global Biogeochem. Cycles *31*, 821-835. https://doi.org/10.1002/2016GB005557.

3. Dow, C., Kim, A.Y., D' Orangeville, L., Gonzalez-Akre, E.B., Helcoski, R., Herrmann, V., Harley, G.L., Maxwell, J.T., McGregor, I.R., McShea, W.J., et al. (2022). Warm springs alter timing but not total growth of temperate deciduous trees. Nature *608*, 552-557. https://doi.org/10.1038/s41586-022-05092-3.

4. Rossi, S., Anfodillo, T., Čufar, K., Cuny, H.E., Deslauriers, A., Fonti, P., Frank, D., Gričar, J., Gruber, A., Huang, J.-G., et al. (2016). Pattern of xylem phenology in conifers of cold ecosystems at the Northern Hemisphere. Glob. Change Biol. *22*, 3804-3813. https://doi.org/10.1111/gcb.13317.

5. Huang, J.-G., Ma, Q.Q., Rossi, S., and Ziaco, E. (2020). Photoperiod and temperature as dominant environmental drivers triggering secondary growth resumption in Northern Hemisphere conifers. Proc. Natl. Acad. Sci. USA *117*, 20645-20652. https://doi.org/10.1073/pnas.2007058117.

6. Huang, J.-G., Zhang, Y.L., Wang, M.H., Yu, X.H., Deslauriers, A., Fonti, P., Liang, E.Y., Mäkinen, H., Oberhuber, W., Rathgeber, C. B. K. (2023). A critical thermal transition driving spring phenology of Northern Hemisphere conifers. Glob. Change Biol. *29*, 1606-1617. https://doi.org/10.1111/gcb.16543.

7. Tamarin-Brodsky, T., Hodges, K., Hoskins, B. J., and Shepherd, T. G. (2020). Changes in Northern Hemisphere temperature variability shaped by regional warming patterns. Nat. Geosci. *13*, 414-421. https://doi.org/10.1038/s41561-020-0576-3.

8. Lewis, S. C., and King, A. D. (2017). Evolution of mean, variance and extremes in 21st century temperatures. Weather. Clim. Extremes *15*, 1-10. https://doi.org/10.1016/j.wace.2016.11.002.

9. Wang, T., Ottlé, C., Peng, S.S., Janssens, I.A., Lin, X., Poulter, B., Yue, C., and Ciais, P. (2014). The influence of local spring temperature variance on temperature sensitivity of spring phenology. Glob. Change Biol. *20*, 1473-1480. https://doi.org/10.1111/gcb.12509.

10. Zohner, C.M., Benito, B.M., Fridley, J.D., Svenning, J.-C., and Renner, S.S. (2017). Spring predictability explains different leaf-out strategies in the woody floras of North America, Europe and East Asia. Ecol. Lett. *20*, 452-460. https://doi.org/10.1111/ele.12746.

11. Vitasse, Y., Lenz, A., and Körner, C. (2014). The interaction between freezing tolerance and phenology in temperate deciduous trees. Front. Plant Sci. *5*, 541. https://doi.org/10.3389/fpls.2014.00541.

12. Delpierre, N., Lireux, S., Hartig, F., Camarero, J.J., Cheaib, A., Čufar, K., Cuny, H., Deslauriers, A., Fonti, P., Gričar, J., et al. (2019). Chilling and forcing temperatures interact to predict the onset of wood formation in Northern Hemisphere conifers. Glob. Change Biol. *25*, 1089-1105. https://doi.org/10.1111/gcb.14539.

13. Zohner, C.M., and Renner, S.S. (2017). Innately shorter vegetation periods in North American species explain native–non-native phenological asymmetries. Nat. Ecol. Evol. *1*, 1655-1660. https://doi.org/10.1038/s41559-017-0307-3.
14. Deslauriers, A., Morin, H., and Begin, Y. (2003). Cellular phenology of annual ring formation of Abies balsamea in the Quebec boreal forest (Canada). Can. J. For. Res. *33*, 190-200. https://doi.org/10.1139/x02-178.
15. Jyske, T., Mäkinen, H., Kalliokoski, T., and Nöjd, P. (2014). Intra-annual tracheid production of Norway spruce and Scots pine across a latitudinal gradient in Finland. Agric. For Meteorol. *194*, 241-254. https://doi.org/10.1016/j.agrformet.2014.04.015.
16. Vitasse, Y., Signarbieux, C., and Fu, Y.S.H. (2018). Global warming leads to more uniform spring phenology across elevations. Proc. Natl. Acad. Sci. USA *115*, 1004-1008. https://doi.org/10.1073/pnas.1717342115.
17. Meng, L., Mao, J.F., Zhou, Y.Y., and Jia, G.S. (2020). Urban warming advances spring phenology but reduces the response of phenology to temperature in the conterminous United States. Proc. Natl. Acad. Sci. USA *117*, 4228-4233. https://doi.org/10.1073/pnas.1911117117.
18. Liu, Q., Piao, S.L., Fu, Y.S.H., Gao, M.D., Peñuelas, J., and Janssens, I.A. (2019). Climatic warming increases spatial synchrony in spring vegetation phenology across the Northern Hemisphere. Geophys. Res. Lett. *46*, 1641-1650. https://doi.org/10.1029/2018GL081370.
19. Cabon, A., Fernández-de-Uña, L., Gea-Izquierdo, G., Meinzer, F.C., Woodruff, D.R., Martí nez-Vilalta, J. and De Cáceres, M. (2020). Water potential control of turgor-driven tracheid enlargement in Scots pine at its xeric distribution edge. New Phytol. *225*, 209-221. https://doi.org/10.1111/nph.16146.
20. Peters, R.L., Steppe, K., Cuny, H.E., De Pauw, D.J.W., Frank, D.C., Schaub, M., Rathgeber, C.B.K., Cabon, A., and Fonti, P. (2021). Turgor—a limiting factor for radial growth in mature conifers along an elevational gradient. New Phytol. *229*, 213-229. https://doi.org/10.1111/nph.16872.
21. Plomion, C., Leprovost, G., and Stokes, A. (2001). Wood formation in trees. Plant Physiol. *127*, 1513-1523. https://doi.org/10.1104/pp.010816.
22. Deslauriers, A., Huang, J.-G., Balducci, L., Beaulieu, M., and Rossi, S. (2016). The contribution of carbon and water in modulating wood formation in black spruce saplings. Plant Physiol. *170*, 2072-2084. https://doi.org/10.1104/pp.15.01525.
23. Verbančič, J., Lunn, J. E., Stitt, M., and Persson, S. (2018). Carbon supply and the regulation of cell wall synthesis. Mol. Plant *11*, 75-94. https://doi.org/10.1016/j.molp.2017.10.004.
24. Busch, F., Hüner, N.P.A., and Ensminger, I. (2007). Increased air temperature during simulated autumn conditions does not increase photosynthetic carbon gain but affects the dissipation of excess energy in seedlings of the evergreen conifer Jack pine. Plant Physiol. *143*, 1242-1251. https://doi.org/10.1104/pp.108.117598.
25. Way, D.A., and Montgomery, R.A. (2015). Photoperiod constraints on tree phenology, performance and migration in a warming world. Plant Cell Environ. *38*, 1725-1736. https://doi.org/10.1111/pce.12431.
26. Thornton, P.K., Ericksen, P.J., Herrero, M., and Challinor, A.J. (2014). Climate variability and vulnerability to climate change: a review. Glob. Change Biol. *20*, 3313-3328.
27. Körner, C., and Basler, D. (2010). Phenology under global warming. Science *327*, 1461-1462. https://doi.org/10.1126/science.1186473.
28. Vitasse, Y., Hoch, G., Randin, C.F., Lenz, A., Kollas, C., Scheepens, J.F., and Körner, C.(2013). Elevational adaptation and plasticity in seedling phenology of temperate deciduous tree species. Oecologia *171*, 663-678. https://doi.org/10.1007/s00442-012-2580-9.
29. Dore, M.H.I. (2005). Climate change and changes in global precipitation patterns: what do

we know? Environ. Int. *31*, 1167-1181. https://doi.org/10.1016/j.envint.2005.03.004.
30. Wang, W.J., Huang, J.-G., Zhang, T.W., Qin, L., Jiang, S.W., Zhou, P., Zhang, Y.L., Peñuelas, J. (2023). Precipitation regulates the responses of xylem phenology of two dominant tree species to temperature in arid and semi-arid forest of the southern Altai Mountains. Sci. Total Environ. *886*, 163951. https://doi.org/10.1016/j.scitotenv.2023.163951.
31. Cuny, H.E., Rathgeber, C.B., Frank, D., Fonti, P., Mäkinen, H., Prislan, P., Rossi, S., Del Castillo, E.M., Campelo, F., Vavrčík, H., et al. (2015). Woody biomass production lags stem-girth increase by over one month in coniferous forests. Nat. Plants *1*, 1-6. https://doi.org/10.1038/nplants.2015.160.
32. Wolkovich, E.M., Davies, T.J., Schaefer, H., Cleland, E.E., Cook, B.I., Travers, S.E., Willis, C.G., and Davis, C.C. (2013). Temperature-dependent shifts in phenology contribute to the success of exotic species with climate change. Am. J. Bot. *100*, 1407-1421. https://doi.org/10.3732/ajb.1200478.
33. Rossi, S., Deslauriers, A., Anfodillo, T., Morin, H., Saracino, A., Motta, R., Borghetti, M. (2006). Conifers in cold environments synchronize maximum growth rate of tree-ring formation with day length. New Phytol. *170*, 301-310. https://doi.org/10.1111/j.1469-8137.2006.01660.x.
34. Rossi, S., Anfodillo, T., and Menardi, R. (2006). Trephor: a new tool for sampling microcores from tree stems. IAWA J. *27*, 89-97. https://doi.org/10.1163/22941932-90000139
35. Fu, Y.S.H., Zhao, H.F., Piao, S.L., Peaucelle, M., Peng, S.S., Zhou, G.Y., Ciais, P., Huang, M.T., Menzel, A., Peñuelas J., et al. (2015). Declining global warming effects on the phenology of spring leaf unfolding. Nature *526*, 104-107. https://doi.org/10.1038/nature15402.
36. Hänninen, H. (1990). Modelling bud dormancy release in trees from cool and temperate regions. Acta Forestalia Fennica *213*, 1-47. https://doi.org/10.14214/aff.7660.
37. Cade, B.S., and Noon, B.R. (2003). A gentle introduction to quantile regression for ecologists. Front. Ecol. Environ. *1*, 412-420. https://doi.org/10.1890/1540-9295(2003)001[0412:AGITQR]2.0.CO;2.
38. Koenker, R., Portnoy, S., Ng, P.T., Melly, B., Zeileis, A., Grosjean, P., Moler, C., Saad, Y., Chwenozhukov, V., Fernandez-Val, I. et al. (2018). Package 'quantreg'. Reference manual available at R-CRAN: https://cran. rproject. org/web/packages/quantreg/quantreg. pdf .
39. Mueller, B., and Seneviratne, S.I. (2012). Hot days induced by precipitation deficits at the global scale. Proc. Natl. Acad. Sci. USA *109*, 12398-12403 https://doi.org/10.1073/pnas.1204330109.
40. Hirschi, M., Seneviratne, S.I., Alexandrov, V., Boberg, F., Boroneant, C., Christensen O.B., Formayer, H., Orlowsky B., and Stepanek, P. (2011). Observational evidence for soil-moisture impact on hot extremes in southeastern Europe. Nat. Geosci. *4*, 17-21. https://doi.org/10.1038/ngeo1032.
41. Bürkner, P.-C. (2017).brms: An R package for Bayesian multilevel models using Stan. J. Stat. Softw. *80*, 1-28. https://doi.org/10.18637/jss.v080.i01.
42. Lefcheck, J.S. (2016). piecewiseSEM: Piecewise structural equation modelling in R for ecology, evolution, and systematics. Methods Ecol. Evol. *7*, 573-579. https://doi.org/10.1111/2041-210X.12512.
43. Nakagawa, S., and Schielzeth, H. (2013). A general and simple method for obtaining R^2 from generalized linear mixed-effects models. Methods Ecol. Evol. *4*, 133-142. https://doi.org/10.1111/j.2041-210x.2012.00261.x.

RESOURCE AVAILABILITY

Lead contact

Further information and requests for resources and reagents should be directed to and will be fulfilled by the lead contact, Jian-Guo Huang

(jianguo.huang@zju.edu.cn).

Materials availability

This study did not generate new unique reagents.

Data and code availability

- Data on the onset dates of cell enlargement, the onset dates of cell wall thickening, site-level temperature variability, precipitation, mean annual temperature, the number of Frost days, chilling and forcing used in the statistical analysis of this study are available as supplemental Excel spreadsheets. DOIs are listed in the key resources table.
- This paper does not report original codes.
- Any additional information required to reanalyze the data reported in this paper is available from the lead contact upon request

EXPERIMENTAL MODEL AND STUDY PARTICIPANT DETAILS

The micro-sampling technique used in our study provides weekly-resolved data of xylogenesis and a detailed firsthand assessment of changes in cell structure, which is an important information that is difficult to collect and mainly been conducted in Europe. Although anatomical methods have been gradually applied in other parts of the world, such as Asia, the data accumulation is still slow since the methods are quite complicated and time-consuming. A massive weekly-resolved xylogenesis data collected from 814 trees that covered boreal, temperate, Mediterranean, and subtropical biomes in North America, Europe, and Asia were used in the current study.

METHOD DETAILS

Field experiments and sample collection

At each site, 1–55 adult dominant trees with upright, healthy stems were selected and sampled throughout the growing season, from January–April to October–December, according to the local climate of the sites and the monitoring years from 1998 to 2016 (Table S1). Wood microcores (2.5 mm in diameter × 25 mm in length) were collected weekly or, occasionally, biweekly from around the stems at breast height (1.3 ± 0.3 m) using a Trephor borer [5,33]. The microcores were then treated according to the protocol described in detail by Rossi et al. (2006) [33].

The sites were distributed across latitudes 23°11′ to 66°12′N and at elevations ranging from 23 to 3,850 m a.s.l. (Fig. S1 and Table S1).

Xylem phenology data

A common protocol was followed for classifying xylem cells at different differentiation phases at all sites. For each sample, the number of cells in the cambial, as well as cells in the enlargement and secondary cell-wall-thickening zones were counted along three radial rows. Cells in different differentiation phases were distinguished using the method explained by Rossi et al. (2006) [33].

The mean number of xylem cells in the enlargement and wall-thickening phases was obtained for each sampling date. The timing of the onset of the cell-enlargement and wall-thickening processes, represented as the day of the year (DOY), was defined for each tree, site, and year as the dates of the appearance of the first radially enlarging and wall-thickening tracheids, respectively, and were referred to as cell-enlargement and cell-wall-thickening DOY.

Climate data

The meteorological stations were installed at 72 sites to measure in situ climate conditions—in a gap in the forest beside or close to the sampled trees. For the remaining 3 sites, we collected data from the nearest meteorological station, NOAA (https://www.ncdc.noaa.gov/cdo-web/datatools/findstation) (Table S1). The temperature values were derived from sensors installed 2–3 m above the ground. The temperature was measured every 15 min and stored in data loggers as hourly averages. From the recorded data, the minimum, mean, and maximum daily temperatures were calculated for further analysis.

Preseason chilling and forcing

Previous studies have used different chilling thresholds for modeling analysis, with daily mean temperatures ranging between 0 °C and 5 °C, −5 and 0 °C, or −10 °C and 0 °C, and found that the temperature range between −5° C and 5° C is the most effective for chilling unit calculation [5]. We calculated preseason chilling accumulation for cell enlargement and wall thickening during the preseason period, corresponding to 80 days before the cell-enlargement and cell-wall-thickening DOY, respectively [35]. In contrast, a temperature threshold above 5° C is the most effective for the forcing unit calculation [5], and we calculated the forcing accumulation for the same preseason periods.

Forcing was computed using a sigmoid function of the average daily air temperature [36]:

$$FU = \sum_{t_0}^{t_d} D_{FU} \qquad if\ T_t > T_{th} \qquad where\ D_{FU} = \frac{28.4}{1 + e^{-0.185(T_t - 18.4)}}$$

Here, FU is the spring forcing unit for the cell-enlargement DOY and cell-wall-thickening DOY, D_{FU} is the daily forcing unit, t_0 is the start date for the forcing accumulation (here, assumed to be January 1st) [5], t_d is the date of appearance of the first wall-thickening cell, T_t is the mean daily air temperature, and T_{th} is the threshold temperature above 5 °C for the forcing accumulation.

Preseason temperature variability (PTV) and frost days

To represent the day-to-day variation in preseason temperature, we adopted the method of Wang et al. (2014) [9], calculating the standard deviation (SD) of mean daily temperatures. The SD was calculated over a specific preseason period for each tree, site, and year, and is hereafter referred to as the PTV. The preseasons were defined as 20, 40, 60, 80, 100, 120, and 140 days before the onset dates of cell enlargement and wall thickening. Therefore, we referred to these PTVs as PTV_{20} to PTV_{140}.

The number of frost days was defined as the days in which the daily minimum temperature was below 0 °C [9] during the selected preseason period, which is the same as the above. We counted the frost days for each tree, site, and year during a specific preseason period.

QUANTIFICATION AND STATISTICAL ANALYSIS

To quantify the range of variations in xylem onset dates (cell enlargement DOY and cell wall thickening DOY) expected from different temperature variability, we performed nonparametric quantile regression analysis instead of conventional least square methods to account for the heterogeneity of data from individual observations [37]. Quantile regression has been widely used for data showing unequal variances in response distributions due to complex interactions between multiple variables, many of which cannot be accounted for [37], and thus allows to avoid assumptions of homoscedasticity and normally distributed errors [38-40]. We fitted multiple quantile levels (1st, 5th, 10th, 15th, 25th, 50th, 75th, 85th, 90th, 95th and 99th

percentiles) of the xylem onset dates as a function of temperature variability in Bayesian hierarchical quantile regression models. We used the asymmetric Laplace distribution implemented in R packages "brms" [41], with sites and species nested within sites as random effects and allowing the effects of temperature variability to vary with tree species to estimate species-specific slopes. We assigned weakly informative priors (normal distribution with mean of zero and standard deviation of ten) for fixed effects to speed up model convergence. The posterior distributions of model parameters were estimated using Hamiltonian Monte Carlo methods by using four chains of 2,000 samples, including 1,000 samples as a warm-up, which was sufficient to achieve adequate mixing and convergence. Thus, a total of 4,000 draws were used to estimate posterior distributions. The convergence and fit of the models were verified by examining the posterior prediction plots (Fig. S2). These probability resampling procedures ensure that the unequal sample size of different sites or species did not affect the regression estimates.

To link observed onset trends of xylem phenology with rising temperature variability, we defined changes in the lower and upper onset dates, represented by the 15% and 85% quantiles of observed cell-enlargement/wall-thickening DOY, respectively. We then used the lower 15^{th} quantile and the upper 85^{th} quantile data for both the cell-enlargement DOY and the cell-wall-thickening DOY to construct four different Structural equation models (SEMs), which generally enable the testing of causal processes that create variations in the onset of cell enlargement and cell wall thickening. We fitted piecewiseSEMs to test the relative importance of the different mechanisms represented by preseason frost days, chilling, and forcing in driving the cell-enlargement DOY and cell-wall-thickening DOY using "piecewiseSEM" package [42]. The marginal and conditional R^2 values, which correspond to the variance of both the fixed and fixed plus random effects (sites and species nested within sites), respectively, were then calculated [43]. We suspect that factors such as local edaphic and topographic factors, geology and vegetational factors were features related to site-specific random effects, which conceivably may interact with temperature variability and could be measured in future studies. Although such factors are technically beyond the present scope of phenological thermal optimum, we expect the inclusion of site-specific random effects to be important both in current and many future studies of spring phenology. We tested whether missing paths exist using Fisher's C statistic, and it is assumed that when the Fisher's C statistic is larger than 0.05 missing paths in the SEM are negligible [42].

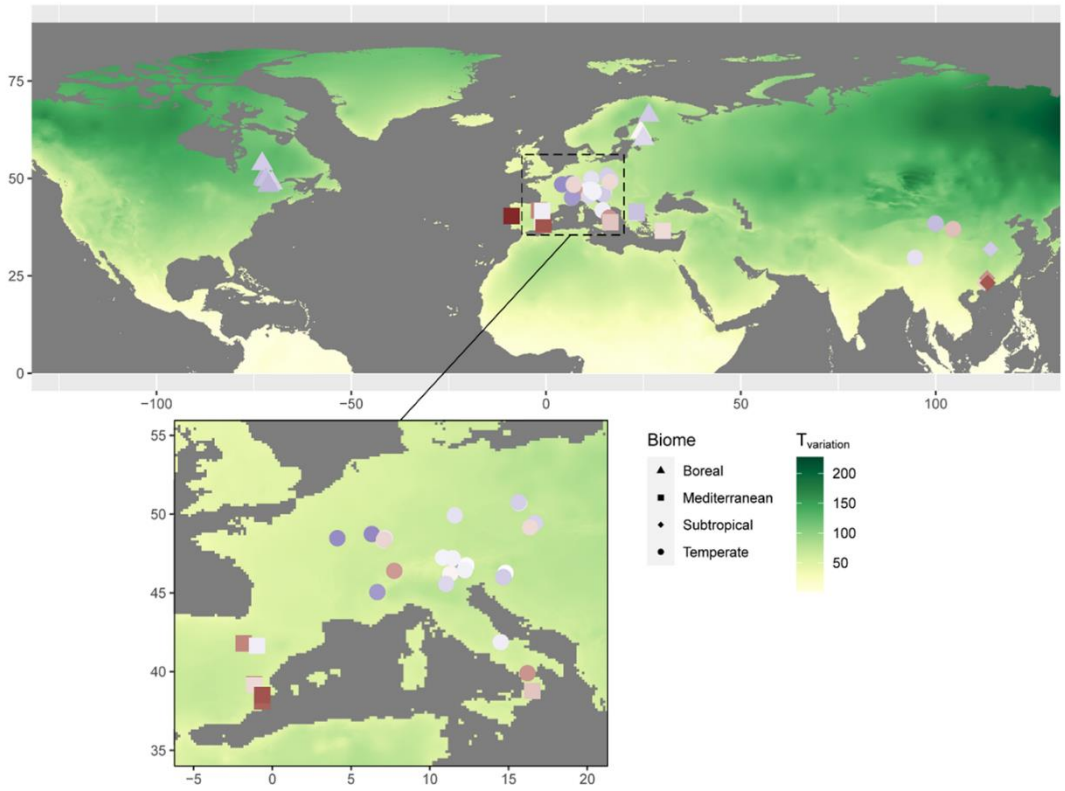

Fig. S1. Location of the study sites across the Northern Hemisphere according to biome type and global temperature variation ($T_{variation}$, obtained from WorldClim Global Climate Data repository using the "bio4-temperature seasonality," spatial resolution: 10'). A high $T_{variation}$ value denotes high temperature variability in certain area for years.

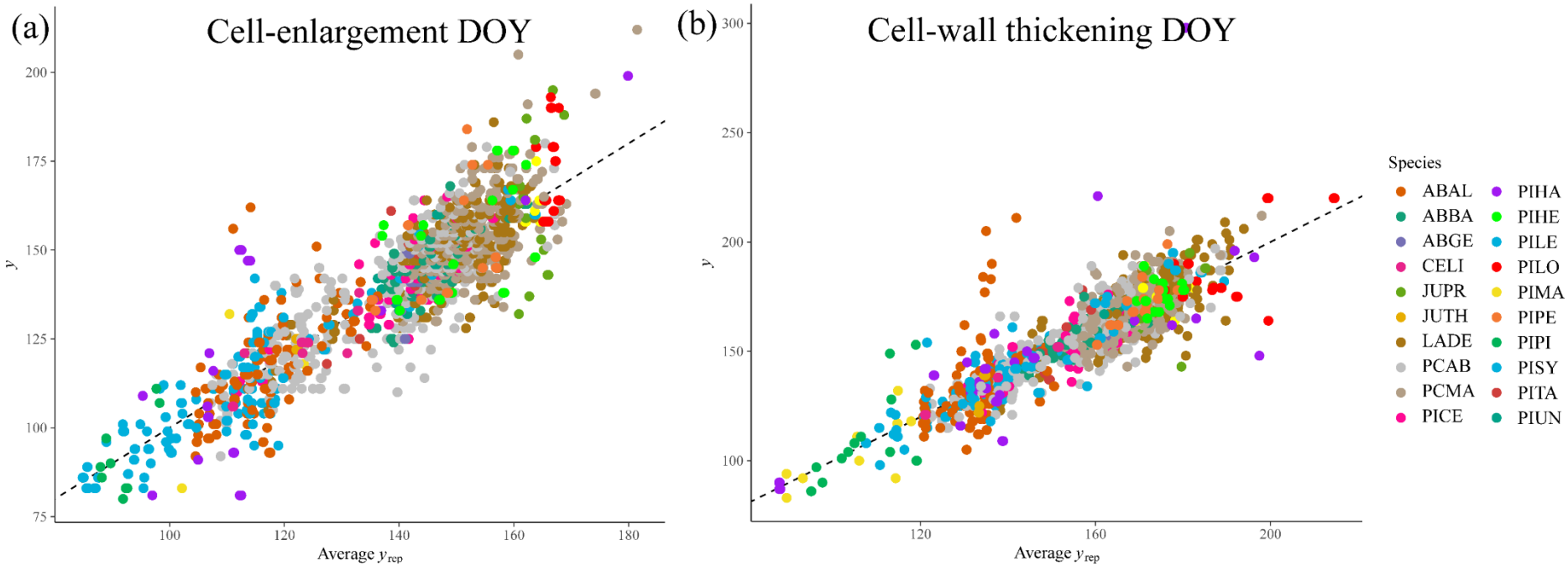

Fig. S2. Scatterplots of the observed data (y) vs the average simulated data (y_{rep}) from the posterior predictive distribution for the species-level. (a) Cell-enlargement DOY; (b) Cell-wall thickening DOY. Dashed line represents a slope of 1.

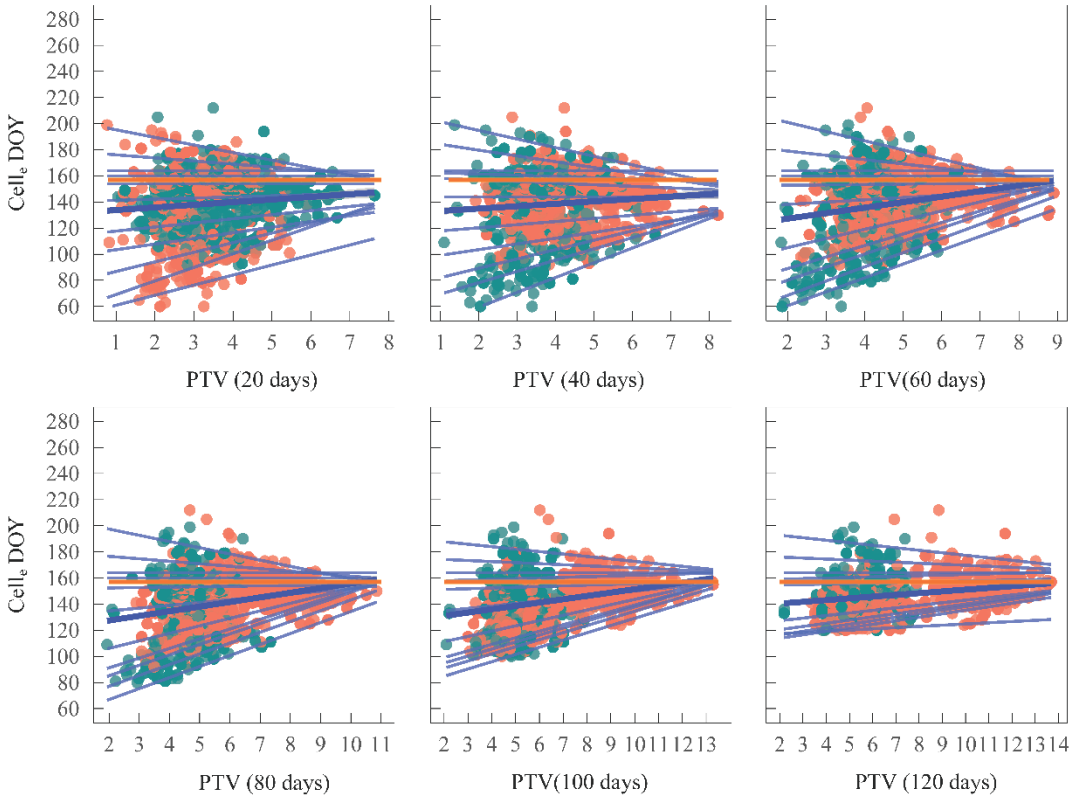

Fig. S3. Plot of the onset dates of cell enlargement (Cell$_e$ DOY) versus the preseason temperature variability (PTV) over different pre-season periods. (A) Pre-season period of 20 days before the **Cell$_e$ DOY**. **(B)** Pre-season period of 40 days before the **Cell$_e$ DOY**. **(C)** Pre-season period of 60 days before the **Cell$_e$ DOY**. **(D)** Pre-season period of 80 days before the **Cell$_e$ DOY**. **(E)** Pre-season period of 100 days before the **Cell$_e$ DOY**. **(F)** Pre-season period of 120 days before the **Cell$_e$ DOY**. **(G)** Pre-season period of 140 days before the **Cell$_e$ DOY**. The red line indicates the Grain-in-Ear; DOY stands for "day of the year." We obtain the median regression with the quantile value of 0.5 (the thick blue line), which can be used as a central regression line similar to the mean regression estimated with OLS regression**.**

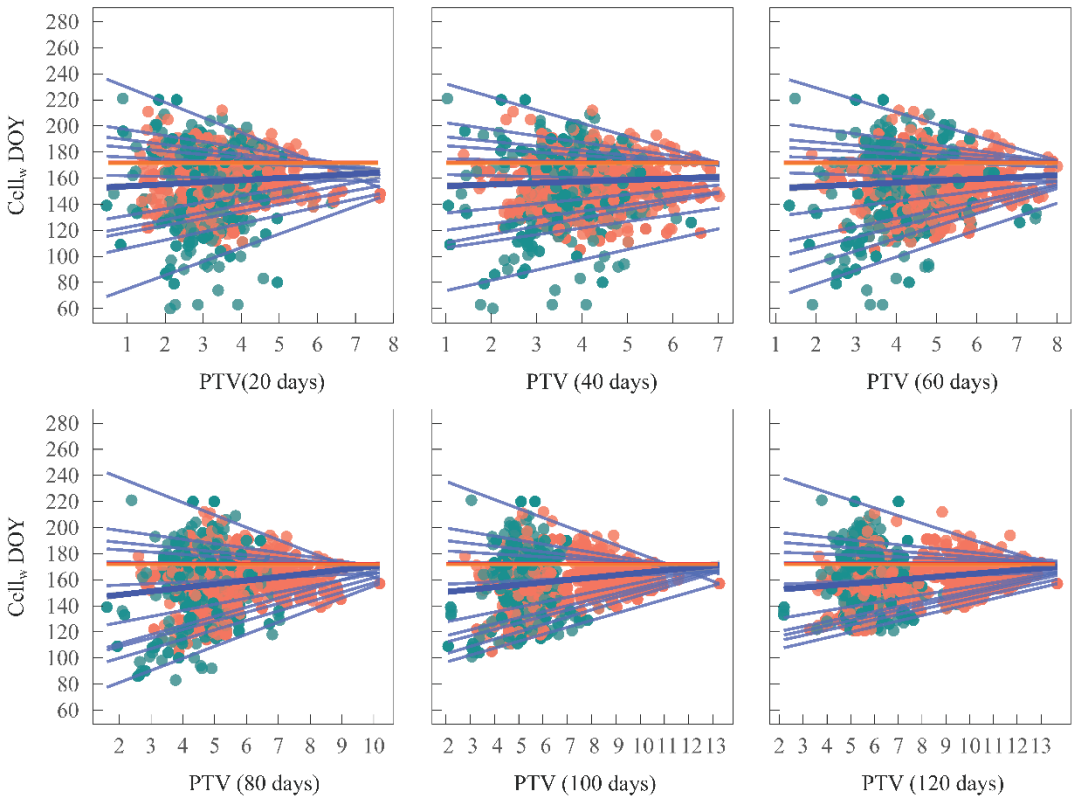

Fig. S4. Plot of the onset dates of wall thickening (Cell$_w$ DOY) versus the preseason temperature variability (PTV) over different pre-season periods. (A) Pre-season period of 20 days before the Cell$_w$ DOY. **(B)** Pre-season period of 40 days before the Cell$_w$ DOY. **(C)** Pre-season period of 60 days before the Cell$_w$ DOY. **(D)** Pre-season period of 80 days before the Cell$_w$ DOY. **(E)** Pre-season period of 100 days before the Cell$_w$ DOY. **(F)** Pre-season period of 120 days before the Cell$_w$ DOY. **(G)** Pre-season period of 140 days before the Cell$_w$ DOY. The red line indicates the summer solstice; DOY stands for "day of the year." We obtain the median regression with the quantile value of 0.5 (the thick blue line), which can be used as a central regression line similar to the mean regression estimated with OLS regression.